LBL-27427
Preprint

Lawrence Berkeley Laboratory
UNIVERSITY OF CALIFORNIA

Materials & Chemical Sciences Division

Submitted to Surface Science

Directed Search Methods for Surface Structure Determination by LEED

P.J. Rous, M.A. Van Hove, and G.A. Somorjai

December 1989

LOAN COPY
Circulates
for 2 weeks
Bldg. 50 Library.
Copy 2
LBL-27427

Prepared for the U.S. Department of Energy under Contract Number DE-AC03-76SF00098.

DISCLAIMER

This document was prepared as an account of work sponsored by the United States Government. While this document is believed to contain correct information, neither the United States Government nor any agency thereof, nor the Regents of the University of California, nor any of their employees, makes any warranty, express or implied, or assumes any legal responsibility for the accuracy, completeness, or usefulness of any information, apparatus, product, or process disclosed, or represents that its use would not infringe privately owned rights. Reference herein to any specific commercial product, process, or service by its trade name, trademark, manufacturer, or otherwise, does not necessarily constitute or imply its endorsement, recommendation, or favoring by the United States Government or any agency thereof, or the Regents of the University of California. The views and opinions of authors expressed herein do not necessarily state or reflect those of the United States Government or any agency thereof or the Regents of the University of California.

LBL-27427

Directed Search Methods For Surface Structure Determination By LEED.

P.J. Rous, M.A. Van Hove and G.A. Somorjai.

Department of Chemistry,
University of California, Berkeley,
and
Center for Advanced Materials,
Materials and Chemical Sciences Division,
Lawrence Berkeley Laboratory,
1 Cyclotron Rd, Berkeley, CA 94720,
U.S.A.

Abstract.

Conventional surface crystallography by Low-Energy Electron Diffraction employs a trial-and-error search controlled at each step by a human being. This trial-and-error approach becomes very cumbersome and unreliable when it is applied to complex surfaces with a large number of unknown structural parameters. We present an automatic optimisation procedure for LEED which combines the complementary techniques of Tensor LEED and a numerical search algorithm. The significant advantages of using Tensor LEED as the basis of a search strategy are illustrated by its application as part of an automatic directed search to the determination of two surface structures: clean Pd(111) and Pd(111) - $(\sqrt{3}x\sqrt{3})$R30^o - CO. This approach can reduce the computer time required for an entire structure determination by several orders of magnitude. It also allows all structural parameters to be found simultaneously; in particular complex, non-symmetric structures and adsorbate induced substrate distortions can be readily determined.

1 Introduction

To date, surface structure determination by LEED (1-3) has suffered from two major theoretical limitations. Both are consequences of the complexity arising from the presence of many independent atoms in the surface unit cell (4,5). Thus, while an a priori structure determination of a simple surface such as Cu(100) can be performed on a microcomputer (6), an organic molecule adsorbed on a catalyst substrate or a complex reconstructed semiconductor surface requires many hours of supercomputer time.

The first limitation is the time taken to perform a single calculation of LEED intensity spectra for a given surface structure which scales as the cube of the number of atoms in the surface unit cell, N^3 , or at best N^2 . Most of the development of LEED theory has concentrated upon this aspect: how to reduce the computational resources needed for a single LEED calculation. This problem has been successfully addressed by a number of reliable approximations to full multiple scattering, which, by the neglect of certain contributions to the scattered intensity, increase the efficiency of a LEED calculation. Examples are Renormalised Forward Scattering (1), Reverse Scattering Perturbation (7), Quasidynamical LEED (8-10) and the Beam Set Neglect method (4,11).

The second , and in many ways more serious, limitation arises from the conventional trial-and-error method of determining a surface structure by LEED, in which human selection of new trial structures is required. This procedure compares the experimental intensity spectra to the results of LEED calculations for a series of trial structures. The actual surface structure is then the trial surface which most closely matches experiment. Usually this is taken to be the surface with the minimum R-factor (3). However, the time taken to perform this trial-and-error search scales exponentially with the number of varied parameters. For example if we wish to determine three structural parameters we must exhaustively explore all corners of a cubic parameter space. The prospects for reliably determining the best fit structure when we are varying as many as 10-20 parameters are clearly limited; most likely

significant regions of such a large volume of parameter space will remain unexplored.

Our solution to these limitations lies in a new approach which attacks both of these problems simultaneously. To this end we have combined Tensor LEED (12-16) with a numerical optimisation algorithm to perform a highly efficient and automatic search for the best fit surface structure. Thus we avoid both the unfortunate N^3 scaling associated with conventional dynamical LEED calculations and the exhaustive trial and error exploration of parameter space .

The idea of using a directed search through parameter space has been suggested since the beginning of quantitative LEED structure determinations (3,17). Indeed, such a search is often used in X-ray crystallography (18). Recently there has been a resurgence of interest in applying a such searches with conventional full dynamical LEED calculations (19,20). One drawback of incorporating a search method into full dynamical LEED is that one is forced to abandon one efficient feature used in such calculations (16,19): the storage of many costly energy dependent quantities which are then used many times to evaluate intensity spectra from a large number of different trial structures simultaneously. For a directed search we need to rapidly evaluate a complete set of intensity spectra at all energies for each trial structure in turn. Thus by attempting to increase the efficiency of the structure determination by using a directed search, the efficiency of the calculation of IV spectra for each trial structure is reduced. Our solution is to use Tensor LEED theory to rapidly evaluate approximate IV spectra, as will be explained in the next section.

Another solution lies in avoiding the structure search altogether and developing a direct method of inverting LEED spectra to yield the surface structure. Such a technique, also based upon Tensor LEED theory, has been proposed and successfully applied to a few simple systems (22). So far, this approach appears to require one to guess the correct atomic coordinates with an accuracy of better than $0.1\mathring{A}$.

2 A Review of The Theory of Tensor LEED.

Tensor LEED is a perturbative approach to the calculation of LEED intensities (12-16). We start by defining a reference structure: a particular surface structure which we guess to be as close as possible to the actual surface structure. We then distort this surface by moving some of the atoms to new positions. In this way we generate a trial structure which is related to the reference structure by a set of atomic displacements. Examples of such a pair of reference and trial surfaces might be an unreconstructed surface and a particular reconstruction, respectively.

To first order, the difference between the amplitudes of a LEED beam scattered from the reference and trial surface, δA can be written as an expression which is linear in the atomic displacements which generate the trial structure. Thus if we move N atoms through δr_{ij} (i=1..N, j=1,2,3):

$$\delta A = \sum_{i=1}^{N} \sum_{j=1}^{3} T_{ij} \delta r_{ij} \tag{1}$$

The quantity T is the tensor which depends only upon the scattering properties of the reference surface and can be calculated by performing what is essentially a full dynamical calculation for this surface. Once T is known then the diffracted intensities for many trial surfaces can be evaluated extremely efficiently by summing [1] after substituting the appropriate set of atomic displacements.

This linear version of tensor LEED is limited to atomic displacements of less than $0.1\mathring{A}$, beyond which [1] becomes a poor approximation. In this case we can appeal to a more sophisticated version of our theory, one which allows displacements of up to $0.4\mathring{A}$ (12-16,23,24), by reformulating eq[1] as:

$$\delta A = \sum_{i=1}^{N} \sum_{L,L'} T_{LL'} R_{LL'}(\delta r_{ij}) \tag{2}$$

$$R_{LL'}(\delta r_{ij}) = j_l(\kappa \delta r_{ij}) Y_{lm}(\delta r_{ij}) j_{l'}(\kappa \delta r_{ij}) Y_{l'm'}(\delta r_{ij}) \tag{3}$$

In eq[2] we have replaced the sum over the three cartesian coordinates with a sum over angular momenta L=(l,m) and L'=(l',m'), the actual displacements of eq[1] being replaced by a function R of those displacements consisting of the product of spherical

Bessel functions and spherical harmonics. For small argument the decrease of the magnitude of the Bessel functions with order effectively cuts off the expansion. This, and the fact that R is a symmetric matrix limits, the number of terms on the LHS of eq[2] to around 37 (25) for the magnitude of atomic displacements for which this equation remains valid. Consequently eq[2] is almost as straightforward as eq[1] to evaluate and is our preferred formula for most situations.

The relative simplicity of the mathematical operations required to evaluate equations [1] or [2] and thus intensities from many trial surfaces has important computational implications. Firstly, the calculation is extremely fast compared to conventional full dynamical methods. By using Tensor LEED theory, the computational time per trial structure can be reduced by a factor of 50 for a simple surface such as Cu(100) to 10,000 for a p(2x2) overlayer system (16). Specfic examples of computer times will be given in section 5. Secondly the time taken to evaluate intensities by Tensor LEED is independent of the presence or lack of symmetry within any given trial surface. Therefore we can consider highly asymmetric systems, such as off-center adsorption sites, with no loss of efficiency. These surfaces are largely inaccesible to conventional methods due to the large volume of parameter space associated with such systems and the inability to exploit symmetries. This is especially important if we are to use an automated structure search since we cannot predict in advance that the path to be taken through parameter space by the optimisation procedure will pass through only symmetrical trial surfaces.

Finally, we can remove a hurdle which has largely prevented the application of automated search methods to conventional LEED. Conventional LEED programs work most efficiently by storing and reusing computationally expensive energy-dependent quantities (such as layer reflection matrices) at a single energy; these are used to evaluate the LEED intensities for as many trial structures as possible- before moving onto the next energy point. In order to implement a directed search we require the reverse. We need a complete set of intensity vs energy spectra for each trial structure in turn. These spectra may be immediately compared to experiment: allowing us to determine the next trial structure to be investigated. Since we can readily store the

tensor T for all energies, this can be done by using Tensor LEED.

These three factors make Tensor LEED ideal as the basis of an automated structure search. The implementation of this procedure in the form of a computer code is discussed in the next section.

3 R-factor Optimisation With Tensor LEED.

Our method is implemented as two separate computer programs. The first program performs the fully dynamical reference structure calculation. The second program takes care of both the trial structure calculations and the search procedure. This is illustrated in the flowchart of figure 1.

The first program generates and stores to disk file one tensor T for each energy point, for each observed beam and for each atom to be displaced from its reference position. The second program reads those tensors and calculates LEED IV spectra for a sequence of trial structures using the tensor LEED theory as expressed by eqs[2] and [3]. The IV spectra of each trial structure examined are immediately compared to the experimental spectra by an in-situ R-factor calculation. We employ a steepest descent method to choose the next trial structure from the results of the previous R-factor comparison, as detailed in the following section. This procedure is repeated until it is determined that an R-factor minimum has been found, at which point the search is terminated.

Of course this method does not guarantee that the trial structure at the termination of the search is the best fit surface structure: this structure may correspond to a local and not the global R-factor minimum (an unavoidable risk with all diffraction techniques). To circumvent this possibility we can repeat the entire optimisation procedure starting with different widely-spaced reference structures which span the parameter space of physically reasonable surface structures. Only one full dynamical calculation is needed for each reference structure, so that the overall computational savings are largely retained. This point is discussed in more detail in section 6.

In addition to determining atomic postions we can also generalise the optimisation

procedure to search for non-structural parameters. This is especially important in the case of the inner potential, variations of which are strongly correlated with the values of all structural parameters. For this reason our optimisation procedure was extended to include the inner potential as an additional parameter to be determined. It is also possible to use Tensor LEED to extend the search to surface properties such as the Debye temperature of each atomic species and anisotropic vibrations in the near-surface region, although such quantities were fixed in the present study.

4 Choosing the Next Trial Structure By Steepest Descent.

In order to select the next trial structure from the results of each R-factor analysis we use a standard numerical optimisation procedure. Since we wish to locate the values of many parameters, the values of which are not constrained, we require a so-called multivariate unconstrained optimisation procedure of which there are many to choose from in the literature (26). For computational ease we selected the Rosenbrook algorithm (26,27), which we have found to be particularly suitable for incorporation into the Tensor LEED codes. This is a sophisticated steepest descent method which requires R-factor evaluations only (derivatives are not required). As with all such procedures it assumes a unimodal function and therefore finds only one function minimum. Briefly, this algorithm proceeds as follows.

Consider a search in which we are attempting to locate the 3N coordinates of N atoms in the surface unit cell. The parameter space we wish to explore has 3N dimensions and any point in this parameter space is uniquely determined by 3N coordinates (X_i) (i=1,2....3N) defined with respect to 3N axes. Initially we choose these axes to be the cartesian coordinates of each atom.

We start the search by selecting an initial trial structure and calculating its R-factor. We then step the first structural variable, X_1 , a distance S_1 . IV spectra are calculated for this structure by Tensor LEED and are compared to the experimental spectra with an R-factor. If the R-factor value has decreased then the move in

designated a success and the corresponding step length, S , is increased by a factor of $\alpha > 1.0$. If the R-factor value increases then the step is reduced by a factor of $\beta < 1.0$ and the step direction is reversed. This procedure is repeated for each of the 3N structural variables in turn until a success followed by a failure have been encountered by all 3N structural parameters. Prior to this stage each structural variable may be changed many times.

We then generate a new set of axes. This is done by defining a rotation matrix M which transforms the old set of axes to the new orthonormal set. The philosophy behind this algorithm is that with each successive rotation of axes we are attempting to orient the axes such that one axis points along the direction of steepest descent while the other axes point in directions along which the change in the R-factor is minimised. Thus, as the search proceeds we "freeze out" certain directions in parameter space and effectively reduce the dimension of the parameter space to be searched. Ultimately, as the search closes in on an R-factor minimum, we approach a one dimensional search, the final location of the minimum corresponding to a reduction to zero dimensions. Thus we successively improve the exponential scaling of the search from t^{3N} , to t^{3N-1} until finally we reach t^0, where t is the time taken for the calculation of IV spectra from a single trial structure .

For the (k+1)th rotation the equations which define the rotation matrix M are as follows;

$$M_{ij}^{(k+1)} = \frac{D_{ij}^{(k)}}{\sum_{i=1}^{3N} \sqrt{D_{ij}^{(k)}}} \tag{4}$$

$$D_{i1}^{(k)} = B_{i1}^{(k)} \tag{5}$$

$$D_{ij}^{(k)} = B_{ij}^{(k)} - \sum_{l=1}^{j-1} \sum_{n=1}^{j} M_{nl}^{(k+1)} B_{nj}^{(k)} M_{il}^{(k+1)} \quad j > 1 \tag{6}$$

$$B_{ij}^{(k)} = \sum_{l=j}^{3N} d_l^{(k)} M_{il}^{(k)} \tag{7}$$

d_i is the total distance moved along the ith axis since the last rotation of axes. At the start of the search M is set to the unit matrix.

Having rotated the axes we search each of the 3N directions of the new coordinate

system starting from the point in parameter space which was reached before the last rotation of axes

$$X_i^{(k+1)} = \sum_{j=1}^{3N} X_j^{(k)} M_{ij}^{(k+1)} \tag{8}$$

The procedure is repeated until further searching yields no significant variation in the structural parameters and/or reduction of the R-factor. At this point the 3N structural parameters define a trial structure corresponding to a local R-factor minimum and the search is terminated.

5 Applications.

5.1 Implementation.

In the following sections we describe that application of our optimisation procedure to two model surfaces: the multilayer relaxation of clean Pd(111) and the determination of the structure of a CO overlayer on Pd(111). Both these surfaces have been the subject of conventional LEED analysis using full dynamical calculation of LEED IV spectra and a trial-and-error search for the best-fit structure. The results of these analyses will be compared to those obtained by our automatic search procedure.

In order to perform these calculations we incorporated the search procedure outlined above as part of our existing TLEED codes. A complete description of these programs is given elsewhere (13,14), but it was necessary, in the case of the CO overlayer system, to extensively modify the previously published versions in order to treat a reference structure with more than one atom in the surface unit cell. To this end we have implemented the composite layer method (2,3) for the reference structure calculation which allows us to treat reference surfaces with an arbitrary number of atoms in the unit cell.

In the following examples the values of all non-structural parameters were the same as those used in the previous full dynamical analysis. The inner potential was optimised for each trial structure to an accuracy of 0.01eV. A single R-factor,

the Pendry R-factor, (28) was used to compare experiment to the results of each trial structure calculation. For the Rosenbrook algorithm it is necessary to select the initial step sizes and the parameters α and β. These were set to $0.05\AA$ for all structural parameters, the values of α and β being 2.0 and 0.5 respectively. We have experimented with the initial choice of these values and have found that provided that these values are reasonable ($0.01 < S < 0.2\AA$, $1.2 < \alpha < 2.0$, $0.2 < \beta < 0.9$) the rate of convergence of the search algorithm is not seriously affected by their magnitude, nor is the location of the correct R-factor minimum.

5.2 Multilayer Relaxations: Pd(111).

In figure 2, we show the results of a directed search in which we attempt to locate the values of the first and second interlayer spacings of Pd(111), d_{12} and d_{23} respectively. In this search we compare the results of Tensor LEED calculations to an experimental data-set measured at normal incidence and consisting of 5 beams between 20 and 300eV, resulting in a cumulative energy range of 700eV (29). The imaginary part of the electron energy was fixed at -5eV and the inner potential optimised simultaneously with the structural parameters. Other structural parameters, such as deeper interlayer spacings, were frozen at their bulk values.

The reference structure was chosen as the bulk termination of Pd(111) in which the interlayer spacing is $d_{12} = d_{23} = 2.250\AA$. Each trial structure was specified by the displacement of the interlayer spacings away from this value, δd_{12} and δd_{23}.

From figure 2 we see that the search rapidly locates the best fit structure for which $\delta d_{12} = +0.096\AA$ and $\delta d_{23} = +0.044\AA$. This structure corresponds to an outward expansion of both the first and second interlayer spacings by 4.3% and 2.0%, respectively. Figure 2 also shows the decrease of the Pendry R-factor (28) as a function of the number of trial structures. We see that after 16 structures the search converges to within $0.004\AA$ of the structure obtained by a full dynamical trial-and-error analysis of the same data set (29). The resulting structure has a Pendry R-factor of 0.159, slightly lower than the value of 0.163 which was obtained by conventional means (which minimised the average of five R-factors, instead of the Pendry R-factor

alone). Also shown in figure 3 is the Pendry R-factor contour plot comparing the experimental data set to the results of a series of full dynamical calculations. This map was obtained from a grid of 100 points spanning the area of parameter space shown. The interpolated R-factor minimum occurs for $\delta d_{12} = +0.092\mathring{A}$ and $\delta d_{23} = +0.042\mathring{A}$, within $0.004\mathring{A}$ of the values determined by our directed search using Tensor LEED. Thus we demonstrate that we are not only locating the correct best-fit surface structure but we also obtain the same result as a full dynamical analysis well within error limits expected of LEED.

The time taken to perform this search with Tensor LEED through 35 structures was 70 CPU seconds on a VAX 8650 computer. This time includes both the in-situ R-factor calculation and optimisation of the inner potential. An additional 69 CPU seconds were required for the reference structure calculation.

5.3 Molecular Adsorption: CO on Pd(111)

Next we used our direct search method to determine the structure of an ordered CO overlayer on Pd(111). We attempted to determine three structural parameters: the CO bond length, the adsorption height and the first interlayer spacing of the Pd substrate. Other structural parameters were frozen, in particular the spacing of all deeper Pd layers was fixed at the bulk interplanar spacing, the CO molecule standing normal to the surface over a fcc hollow site.

The experimental data-set consisted of 8 beams taken at normal incidence between 20 and 200eV with a cumulative energy range of 700eV (29). The reference structure, shown schematically in figure 4a, was taken to have a CO bond length equal to $1.10\mathring{A}$ and an adsorption height of $1.1\mathring{A}$. The top interlayer spacing of the substrate was taken as its bulk value of $2.250\mathring{A}$. Figure 5 shows the progress of the search as a function of the number of trial structures examined. The search converges after approximately 40 structures have been explored, the Pendry R-factor falling from 0.87 to 0.55. The best fit structural parameters, shown schematically in figure 4b are: a CO bond length of $1.16\mathring{A}$, and adsorption height of $1.26\mathring{A}$ and a change of the top interlayer Pd spacing to $2.39\mathring{A}$ corresponding to a 6% expansion. These values are

within 0.03Å of the results of a full dynamical trial-and-error search (29) for which CO bond length was 1.15Å, and adsorption height 1.29Å and the top interlayer Pd spacing expanded to 2.386Å. The minimum value of the Pendry R-factor was also 0.55. (in the conventional calculation the structure was optimised using a five R-factor average rather than the Pendry R-factor alone).

The CPU time required for this search through 60 structures was 290 CPU seconds on a VAX 8650 computer. An additional 240 CPU seconds were required for the reference structure calculation.

6 Discussion and Conclusions.

We have presented the results of a new combined approach to surface structure determination by LEED. By coupling the calculation of IV spectra by Tensor LEED with a numerical optimisation algorithm we have achieved a practical solution to many of the problems encountered with conventional structure determination. This method appears to be able to reproduce the results obtained by full dynamical trial-and-error methods but with an efficiency increased by several orders of magnitude. Indeed the speed of this technique implies that it is now possible to determine even complicated structures interactively on a small computer. An important advantage of this method is that many more structural and non-structural parameters can be fitted to experiment than before. This allows us to avoid the usual temptation of assuming high-symmetry structures or ignoring the potential distortion of a substrate induced by an adsorbed atom or molecule.

A limitation of the Tensor LEED approach is that the guessed reference structure must have structural parameters well within 0.4Å of those of the best-fit structure (12,16). Many surface structures fall within this category (for example, clean-surface relaxations or surfaces with reasonably well-known structures). Then the final structural result of our method is sufficiently close to the initial guess that no further analysis is necessary. This is the most desirable and efficient case, which applies to the examples described in Section 5.

In less immediate cases, our method may yield structural parameters that are more than 0.2Å away from those in the reference structure. Then their accuracy is doubtful and it becomes necessary to start a new search around that first result. This requires a second fully-dynamical calculation with the first result as a new reference structure. This procedure may have to be repeated if the latest result is found to lie still farther away.

For more complex structures, where one has little a priori knowledge of atomic positions, a similar iterative approach is indicated. One would iteratively find new structural "guesses" and start fresh directed searches with Tensor LEED from each new reference structure in turn. The process will inevitably reach a minimum in the R-factor, representing a best-fit structure. Whether this is the globally-best structure will be discussed below. It is however important to realise that one only performs full multiple-scattering calculations once at each iterative step, still an immense improvement over conventional trial-and-error searches.

A special case is the determination of an adsorption site, such as top vs. bridge vs. hollow site. Then the interatomic distances are often easily guessed and mild substrate relaxations are expected. The distance between distinct adsorption sites is normally, however, far larger than the 0.4Å limit of the validity of Tensor LEED, and one cannot rely on the R-factor function to decrease monotonically from an incorrect site to a correct site. It is, in any event, simpler to make a good guess for the structure in each adsorption site, make one full dynamical reference structure calculation for each site and start seperate directed searches from each site. The best R-factor among the sites solves the structure.

We must now address the issue of global vs. local R-factor minima (30), since it is well known that many local minima can arise with diffraction techniques. The critical question here is how far apart different minima are located in structural parameter space. If minima occur close together, many local minima will have to be found and explored one by one, an obviously undesirable situation. A few well-separated minima can be explored much more efficiently. (We must assume here that we can confine our structural search to a finite region of parameter space, defined by reasonable bonding

configurations; otherwise an infinite number of possible minima would prevent any structure determination with any search scheme.)

The distance between R-factor minima is determined firstly by the diffraction conditions, i.e. wavelength as well as incident and emergent directions. This is most easily seen in the kinematic limit. Let us gradually move an atom by a growing displacement dr away from an R-factor minimum. We let the motion change the scattered-wave phase $\delta k.\delta r$ by up to 2π, where δk is the momentum transfer to a particular emergent beam. During this move the beam intensity changes until it reverts to its original value. An R-factor using that intensity alone would increase and then decrease back to its original minimum value. More realistic R-factors that average over many energies and beams would also exhibit oscillations on the same scale of displacements. Multiple scattering also would not affect this scale.

The scale for the distance between R-factor minima due to diffraction is therefore set by practical values of δk. For LEED, one obtains typically about $0.5\mathring{A}$ for atomic displacements perpendicular to the surface. For displacements parallel to the surface one obtains larger values, such as $1\mathring{A}$ or more (this scale depends inversely on the component of δk parallel to the surface).

Secondly, smaller distances between R-factor minima can occur when atoms move in concert rather than individually, as we have assumed up to now. For example, shrinking the size of a molecule will cause faster R-factor variations because more atoms move at the same time. Closer R-factor minima can occur in particular when averaging over symmetrically-equivalent rotated or mirrored domains: then equivalent atoms move simultaneously in symmetrically-equivalent directions in different domains. For instance, if an adatom prefers to sit asymmetrically away from a site that has n-fold rotational symmetry, then one must expect n R-factor minima in n directions around that symmetrical site, at whatever small or large distance the atom chooses to be from that site. Thus, correlated motion can cause closely-spaced R-factor minima. The more complex the structure, the more opportunities for local minima one must expect. This applies especially to low-symmetry structures where small displacements can occur in many directions. Only experience will tell how best

to handle such cases.

A structural search method has no alternative but to explore all plausible R-factor minima and find the deepest one. This applies also to our directed search method. Thus one should in general try out blindly (or preferably with educated guesses) a number of reference structures in order to identify the various minima, before discriminating between them based on their respective R-factor values. Our scheme, however, remains very attractive compared to any conventional trial-and-error approaches, since it only requires one full dynamical calculation for each reference structure. In addition, due to the nature of Tensor LEED, all possible atomic displacements are accessible equally efficiently.

The alternative to performing a structure search is the development of a direct method of inverting LEED intensities to yield the surface structure in the same manner that Fourier transform and phase retrieval techniques are used in X-ray crystallography (18). With LEED it is impossible to determine directly the atomic positions from first principles in this way because the strong electron scattering means that there is no direct analytic relationship linking the atomic positions and the scattered wavefield. However, Tensor LEED does provide a simple relationship between the changes in LEED intensities and the structural distortions that cause them.

Thus by considering the difference between measured intensities and those calculated for a reference surface it seems to be possible to invert eq[1] and directly determine the correct surface structure,at least for displacements of less than $0.1\mathring{A}$ (22). It remains to be seen whether this new method can be applied to more complex surfaces such as adsorbate systems, but is mentioned here as a potential alternative to the methods presented here.

Acknowledgements.

P.J.R thanks the U.K. Science and Engineering Research Council for continued support through the award of a Postdoctoral Research Fellowship. The experimental part of this work was supported by the Director, Office of Energy Research, Office of

Basic Energy Sciences, Materials Science Division of the US Department of Energy under Contract No. DE-AC03-76SF00098. Supercomputer resourses were provided by the Office of Energy Research of the Department of Energy.

References

1. J.B. Pendry, *Low Energy Electron Diffraction* (Academic, New York, London, 1974).

2. M.A. Van Hove and S.Y. Tong, *Surface Crystallography By LEED* (Springer, Berlin, Heidelberg, New York, 1979).

3. M.A. Van Hove, W.H. Weinberg and C.M. Chan, *Low Energy Electron Diffraction* (Springer, Berlin, Heidelberg, New York, 1986)

4. M.A. Van Hove, in *Chemistry and Physics of Solid Surfaces VII*, Eds R.F. Howe and R. Vanselow (Springer, Berlin, Heidelberg, New York, 1988), p513.

5. K. Heinz, Prog. Surface. Sci. **27** (1988) 239.

6. N Bickel and K. Heinz, Surface. Sci. **163** (1985) 435.

7. R.S. Zimmer and B.W. Holland, J. Phys. **C8** (1975) 2395.

8. D. Aberdam, R. Baudoing and C. Gaubert, Surface. Sci. **52** (1975) 125.

9. S.Y. Tong, M.A. Van Hove and B.J. Mrstik, *Proc. 7th. Intl. Vac. Cong. and 3rd Intl. Conf. on Surface Science* (Vienna,1977), p2407.

10. K. Heinz and G. Besold Surface. Sci. **125** (1983) 515.

11. M.A. Van Hove, R.F. Lin, and G.A. Somorjai, Phys Rev Lett. **51** (1983) 778.

12. P.J. Rous, J.B. Pendry, D.K. Saldin, K. Heinz, K. Müller and N. Bickel, Phys. Rev. Lett. **57** (1986) 2951.

13. P.J. Rous and J.B. Pendry, Comput. Phys. Commun. **54** (1989) 137.

14. P.J. Rous and J.B. Pendry, Comput. Phys. Commun. **54** (1989) 157.

15. P.J. Rous and J.B. Pendry, Surface Sci (in print).

16. P.J. Rous and J.B. Pendry, Surface Sci (in print).

17. D.L. Adams , *Proceedings of the First International Seminar on Surface Structure Determination By LEED*, Erlangen 1985.

18. G.H. Stout and L.H. Jensen, *X-Ray Structure Determination*, (Macmillan, New York, 1968).

19. P.G. Cowell, M. Prutton, S.P. Tear, Surface Sci **177** (1986) L915

20. P.J. Rous and J.B. Pendry, in *The Structure of Surfaces II*, Ed. J.F. van der Veen and M.A. Van Hove (Springer, Berlin, Heidelberg, New York, 1988)

21. G. Kleine, W. Moritz, D.L. Adams and G. Ertl, Proceedings of the 10th European Conference on Surface Science (ECOSS-10), Bologna 1988, to be published in Surface. Sci.

22. J.B. Pendry, K. Heinz and W Oed, Phys. Rev. Lett. **61** (1988) 2953.

23. N. Bickel, K. Heinz, H. Landskron, P.J. Rous, J.B. Pendry and D.K. Saldin, in *The Structure of Surfaces II*, Ed. J.F. van. der Veen and M.A. Van Hove (Springer, Berlin, Heidelberg, New York, 1988)

24. J.B. Pendry, K. Heinz, W. Oed, H. Landskron, K Müller and G. Schmidtlein, Surface. Sci. **193** (1988) L1.

25. P.J. Rous, Submitted to Comput. Phys. Commun. August 1989.

26. J.L. Kuestler and J.H. Mize, *Optimization Techniques With Fortran* (McGraw-Hill, New York, St Louis, San Francisco, 1973).

27. H.H. Rosenbrook, Computer. J. **3** (1960) 175.

28. J.B. Pendry, J. Phys **C13** (1980) 937.

29. H. Ohtani, M.A. Van Hove and G.A. Somorjai, Surface. Sci. **187** (1987) 372.

30. One class of optimisation algorithm that can find global minima, at the expense of many function evaluations, is optimisation by simulated annealing. The large number of function evaluations required by this technique presently rules out its application to the LEED problem, even if we use Tensor LEED theory. A discussion of the advantages and disadvantages of this method can be found in: W.H. Press, B.P. Flannery, S.A. Teukolsky, W.T. Vetterling, *Numerical Recipes*, (Cambridge University Press, 1986)

Figure Captions

Figure 1. A flowchart for R-factor optimisation by Tensor LEED. The reference structure calculation is a self-contained program which generates the tensors T for the best guess structure. The remainder of the calculation is performed by a single program which combines the calculation of IV spectra by Tensor LEED and in-situ R-factor optimisation.

Figure 2. The evolution of the structural parameters δd_{12} (upper panel) and δd_{23} (centre panel) and the Pendry R-factor (lower panel) as a function of the number of trial structures investigated in a directed search applied to Pd(111). The reference structure was the bulk termination of the solid for which δd_{12} and δd_{23} = 0.0. The search converges after investigating approximately 15 structures at which point δd_{12}=+0.096$\AA$, δd_{23}=+0.044$\AA$ and R_p=0.159. The result of a full dynamical trial-and-error analysis is indicated by the black dots at δd_{12}=+0.092$\AA$, δd_{23}=+0.042$\AA$ and R_p=0.163.

Figure 3. Pendry R-factor map comparing the results of 100 full dynamical calculations to experimental IV spectra for Pd(111) for a range of top and second interlayer spacings. The interpolated R-factor minimum of 0.163 occurs at δd_{12}=+0.0.092$\AA$ and δd_{23} =+0.042$\AA$. The path of the automatic search algorithm (also shown in figure 2) is indicated.

Figure 4a. A schematic diagram of the reference structure used to intialise the directed search for the Pd(111) - $(\sqrt{3}x\sqrt{3})$R30° - CO surface.

Figure 4b. A schematic diagram of the best-fit trial structure located by the directed search for the Pd(111) - $(\sqrt{3}x\sqrt{3})$R30° - CO surface. structure.

Figure 5. The progress of the directed search to obtain the surface structure of Pd(111) - $(\sqrt{3}x\sqrt{3})$R30° - CO. The top interlayer spacing of the substrate, the CO bond length and the adsorption height are monitored as a function of the number of trial structures examined. After approximately 40 structures have been investigated, the search converges close to the results of a full dynamical trial and error search which are indicated by the black dots.

A Directed Search With Tensor LEED

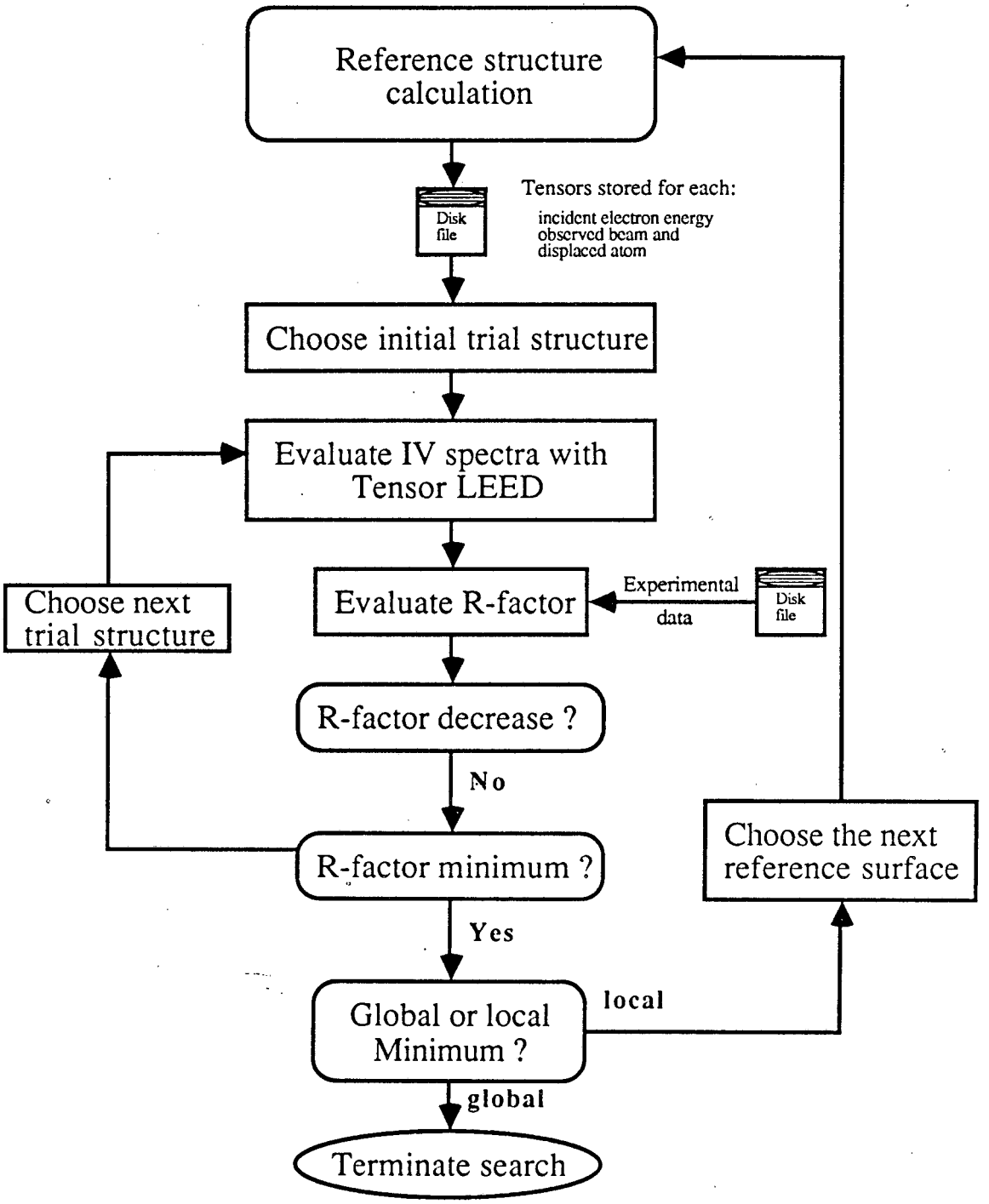

XBL 896-2272

Fig. 1

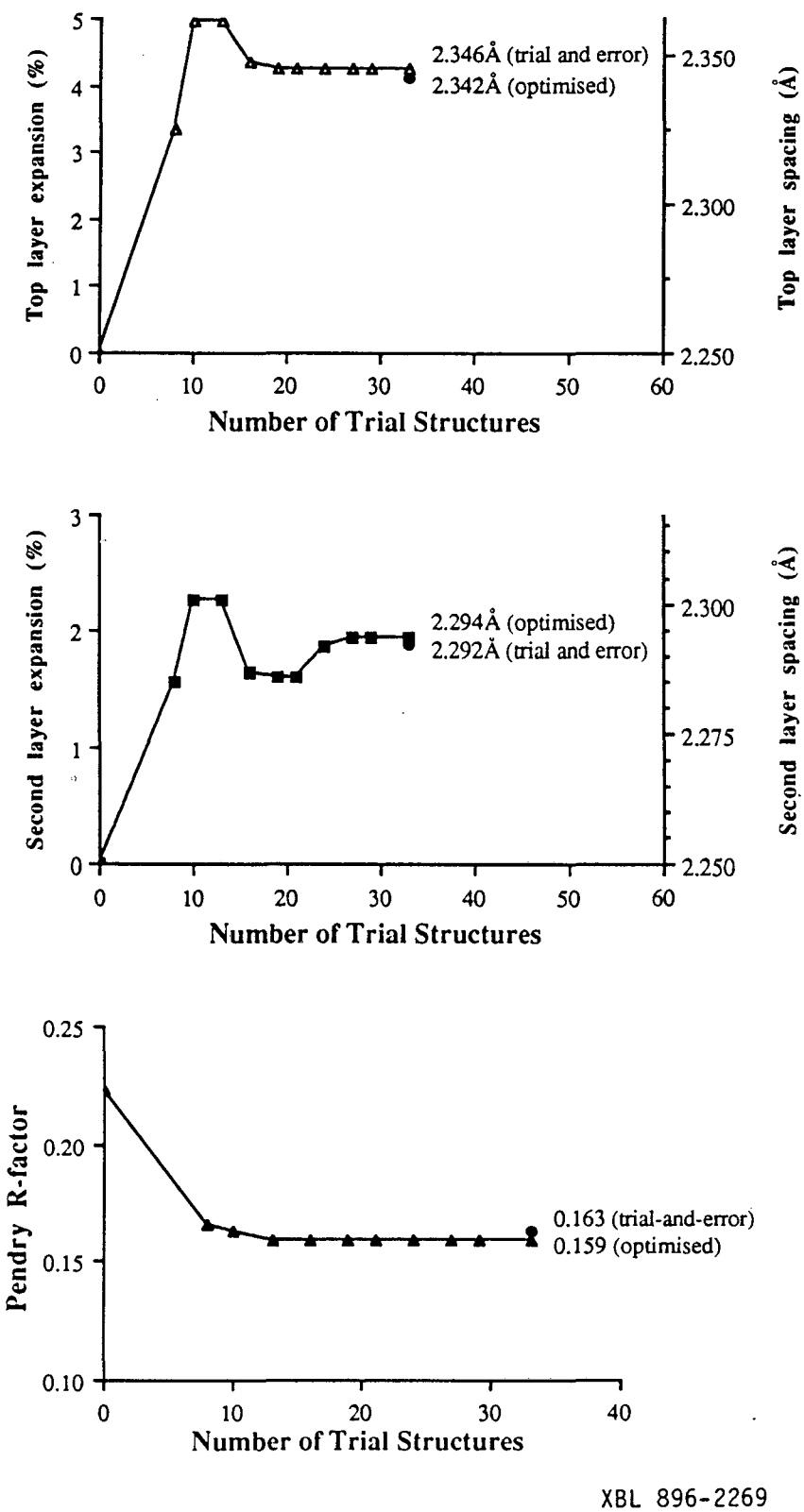
Top layer expansion (%)
Top layer spacing (Å)
2.346Å (trial and error)
2.342Å (optimised)
Number of Trial Structures
Second layer expansion (%)
Second layer spacing (Å)
2.294Å (optimised)
2.292Å (trial and error)
Number of Trial Structures
Pendry R-factor
0.163 (trial-and-error)
0.159 (optimised)
Number of Trial Structures
XBL 896-2269

Fig. 2

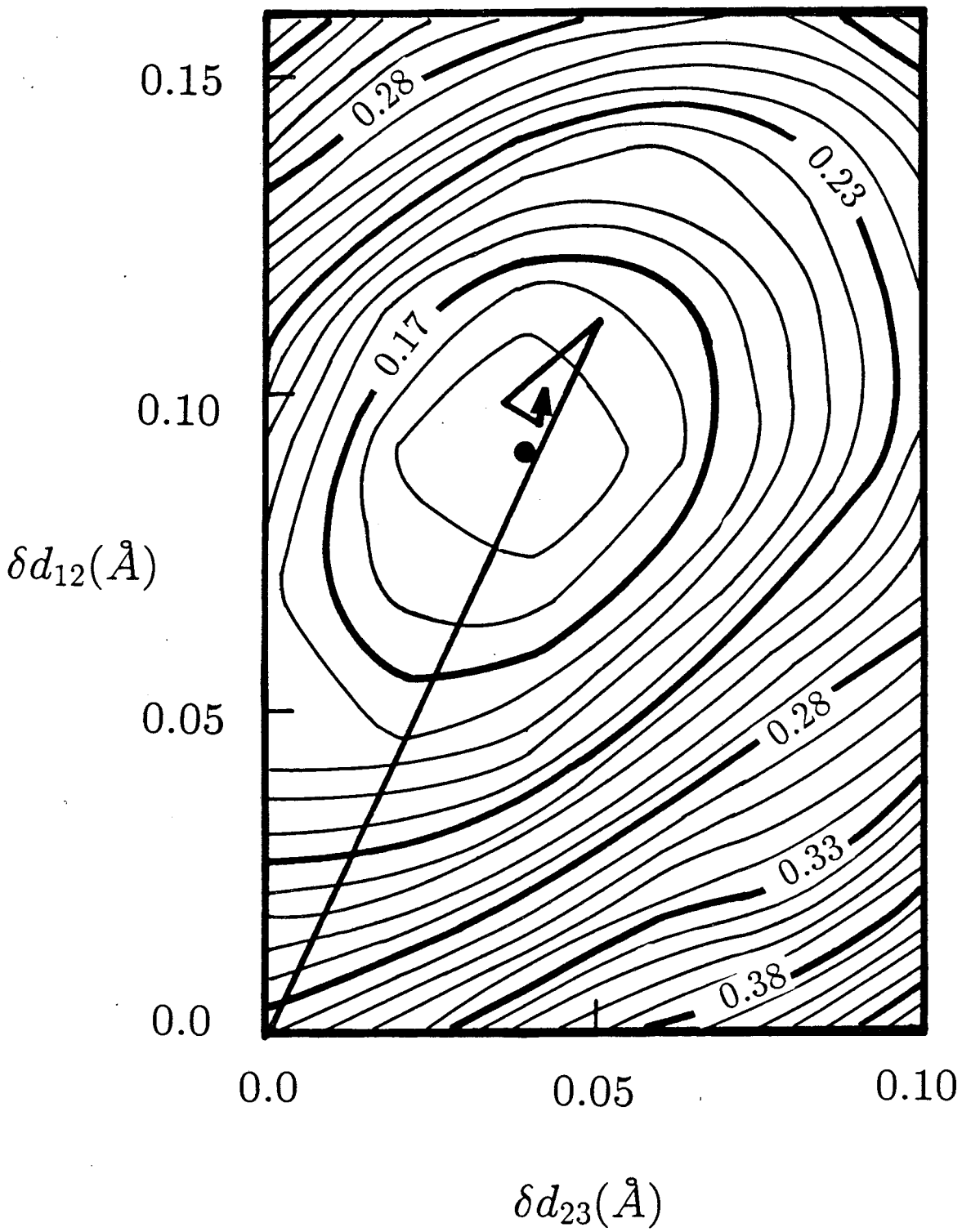

XBL 896-2274

Fig. 3

Pd(111)-(√3X√3)R30°-CO

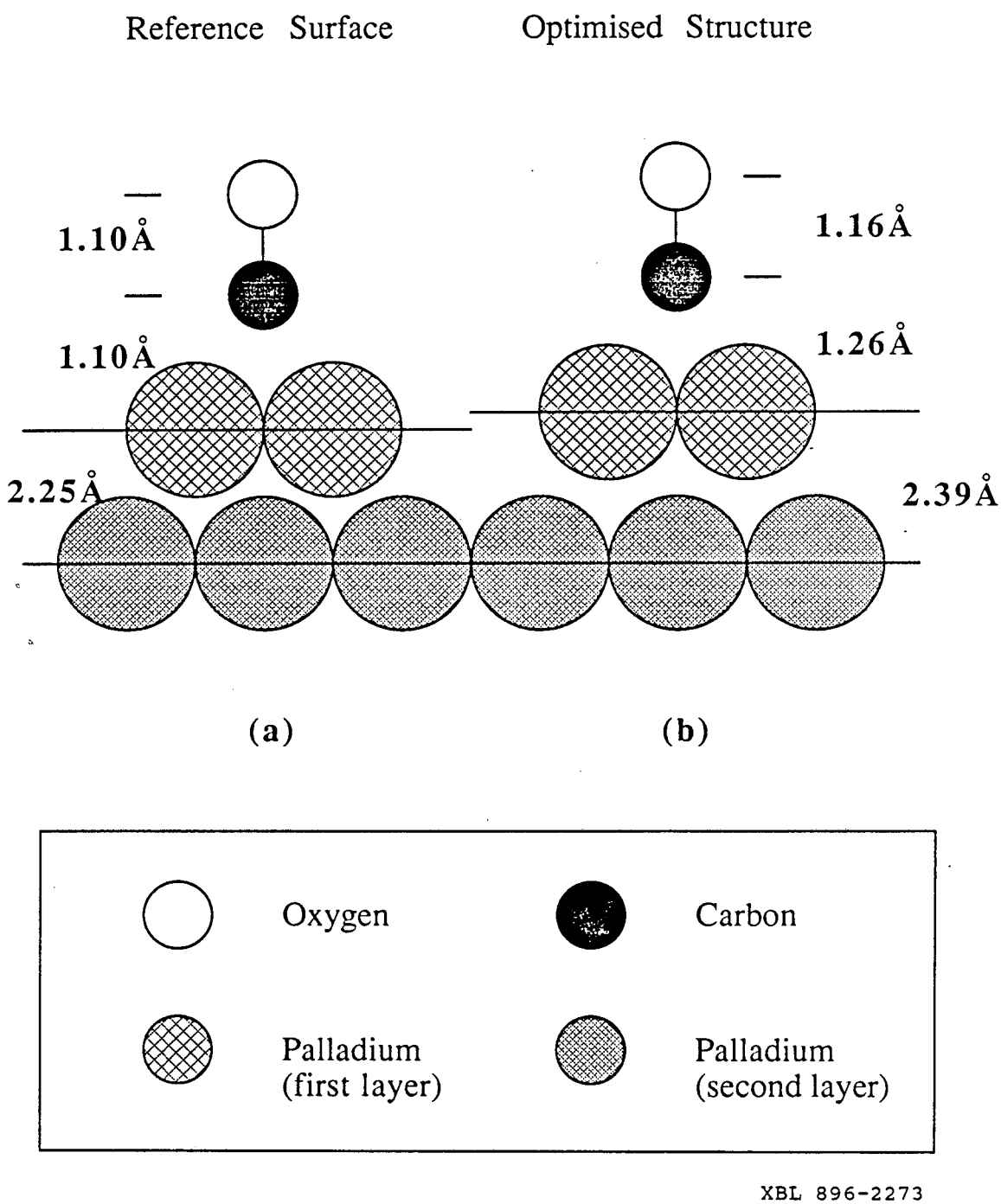

Fig. 4

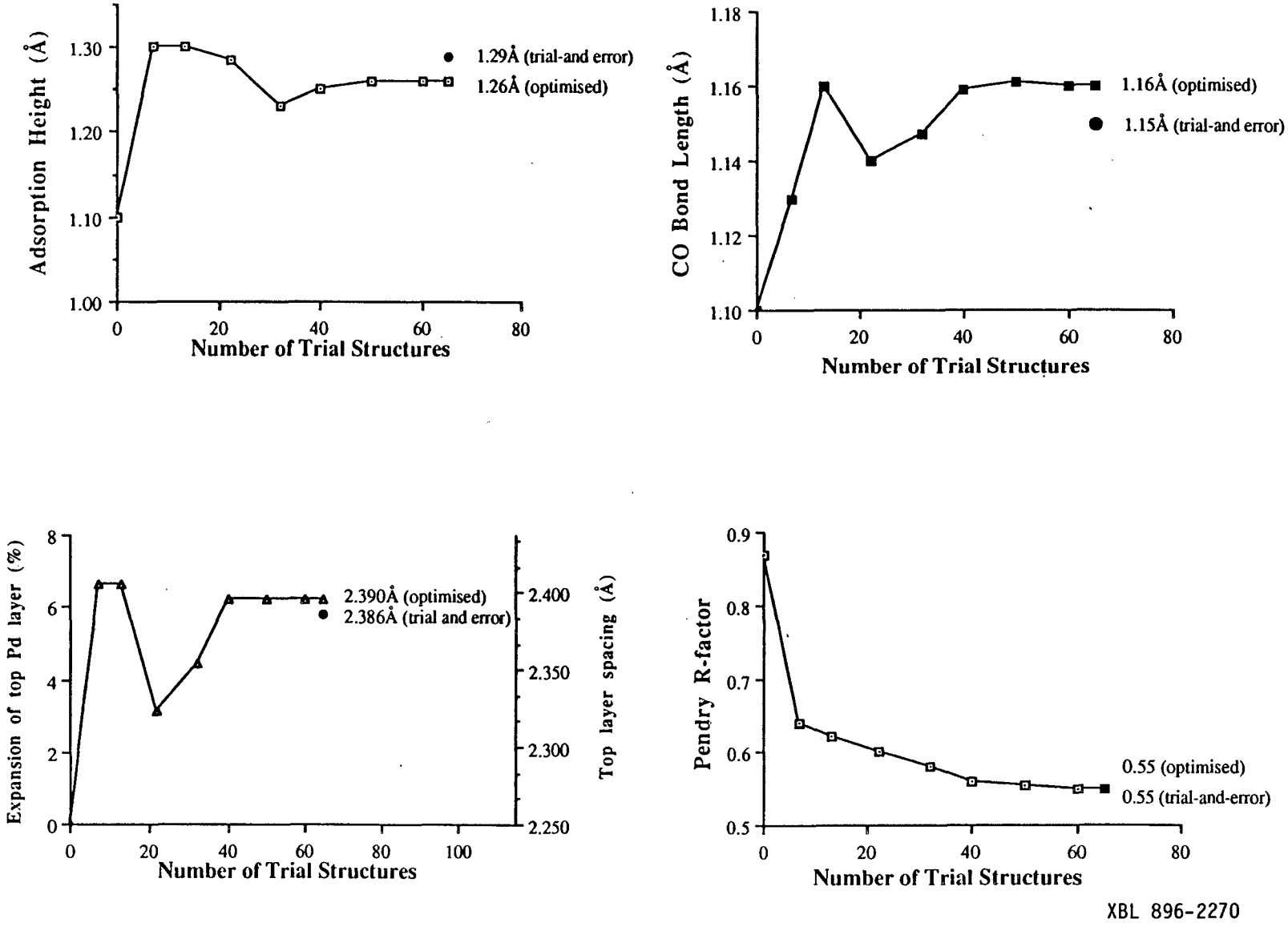
Adsorption Height (Å)
1.30
1.20
1.10
1.00
0
20
40
60
80
Number of Trial Structures
1.29Å (trial-and error)
1.26Å (optimised)
CO Bond Length (Å)
1.18
1.16
1.14
1.12
1.10
0
20
40
60
80
Number of Trial Structures
1.16Å (optimised)
1.15Å (trial-and error)
Expansion of top Pd layer (%)
8
6
4
2
0
0
20
40
60
80
100
Number of Trial Structures
2.390Å (optimised)
2.386Å (trial and error)
Top layer spacing (Å)
2.400
2.350
2.300
2.250
Pendry R-factor
0.9
0.8
0.7
0.6
0.5
0
20
40
60
80
Number of Trial Structures
0.55 (optimised)
0.55 (trial-and-error)
XBL 896-2270

Fig. 5

LAWRENCE BERKELEY LABORATORY
TECHNICAL INFORMATION DEPARTMENT
1 CYCLOTRON ROAD
BERKELEY, CALIFORNIA 94720